Influence of Seed Polymer Molecular Weight on Polymerization Kinetics and Particle Morphology of Structured Styrene–Butadiene Latexes

OLA J. KARLSSON, HELEN HASSANDER, BENGT WESSLÉN

Department of Polymer Science & Engineering, Lund Institute of Technology, P.O. Box 124, SE-22100 Lund, Sweden

Received 8 June 1998; accepted 22 August 1999

ABSTRACT: Heterogeneous film-forming latexes were prepared using two-stage, seeded emulsion polymerization. The polymerization was performed in a calorimetric reactor with a control unit that monitored the reaction rate and controlled the charging rate of the monomers. Three types of styrene seed latexes were prepared at 70°C. The first was an unmodified polystyrene (PS) latex. The second had the molecular weight lowered by the use of carbon tetrachloride (CCl_4) as a chain-transfer agent, added at the start of the polymerization. For the third one, divinylbenzene (DVB) was used as a comonomer. DVB was added under starved conditions near the end of the polymerization to achieve crosslinked particle shells and to introduce double bonds as possible grafting sites. The second polymerization step was performed at 80°C as a batch operation in a 200-mL calorimeter reactor. The second-stage polymer was poly(styrene-*co*-butadiene-*co*-methacrylic acid) (S/B/MAA). A fixed S/B ratio was used together with varying small amounts of MAA. Particle morphology and particle-size distributions were examined after the second stage using TEM after staining with osmium tetroxide. The particle morphology was found to depend on both the seed composition and the amount of MAA used in the second stage. Molecular weight and crosslinking of the DVB-containing seed influenced the internal particle viscosity, which gave differences in the polymerization rate and the particle morphology. Crosslinking of the second-stage polymer decreased the monomer concentration in the particles, which could be detected as a change in the slope the pressure/conversion curve. This phenomenon was used to indicate the critical conversion for crosslinking of the second-stage polymer. © 2000 John Wiley & Sons, Inc. J Appl Polym Sci 77: 297–311, 2000

Key words: two-stage; seeded emulsion polymerization; calorimetric reactor; particle viscosity; monomer vapor pressure; particle morphology; core–shell

INTRODUCTION

Styrene–butadiene (S/B) copolymer latexes are widely used as binders in paper and board coatings. In the paper industry, the binders generally contain between 30 and 50% B by weight, because an optimal balance of coating strength[1] and optical and printing properties[2] are obtained in this region. Although the binder is used in small amounts in the final coating, the film-forming ability as well as the physical and mechanical properties of the binder is of great importance for the coating performance. A combination of low film-forming temperature and high modulus and stiffness at ambient temperature is difficult to obtain with conventional S/B latexes. However,

Correspondence to: B. Wesslén (bengt.wesslen@polymer.lth.se).

Contract grant sponsor:Swedish Research Council for Engineering Sciences, TFR.

Journal of Applied Polymer Science, Vol. 77, 297–311 (2000)

heterogeneous latexes offer these binder properties.[3,4]

Heterogeneous latex particles with different particle morphologies can be prepared by two-stage emulsion polymerization. When the second-stage monomer is different from that used for the seed polymer, phase separation occurs and many types of heterogeneous morphologies may be formed.[5–14] It is also possible to obtain latexes with a wide range of physical and mechanical properties for a given combination of monomers by using different polymerization techniques.[15–24] The film-forming properties of latex depend on the particle morphology and the surface properties. Parameters such as the relative hydrophilicity[10,13,14,25–33] of the different polymer phases and the internal particle viscosity[7,14,27,33–37] during polymerization have a great influence on the particle morphology.

The internal particle viscosity is closely related to the polymer molecular weight[13,34,35] and to the crosslink density in the seed particles.[13,38–40] Even low crosslink densities can greatly influence the latex particle morphology.[41] Several authors have proposed models based on general thermodynamic and kinetic considerations to explain and predict particle morphologies in seeded emulsion polymerization.[35,42–52]

In a series of articles, we presented results from the preparation of heterogeneous S/isoprene and S/B latex particles.[4,14,24,53,54] In the present work, the aims were to find relations between, on the one hand, the molecular weight and the crosslink density of the seed polymer and, on the other, the reaction kinetics of the second stage of a seeded emulsion polymerization. Furthermore, the particle morphologies were to be studied. Polystyrene (PS) latexes with different molecular weights and crosslinking densities were prepared and used as seeds for a second-stage copolymerization of B, S, and varying small amounts of methacrylic acid (MAA). A pressurized calorimetric reactor equipped with pressure transducers was used, which allowed close monitoring of the polymerization rates and monomer consumption. The molecular weights of the polymers were determined by gel permeation chromatography (GPC), monitored by light scattering (LALLS) and viscometry detectors. The final particle morphologies were examined with TEM after staining with osmium tetroxide.

THE CALORIMETRIC REACTOR

Pressurized calorimetric reactors of two sizes were used: a 2-L reactor (ChemiSens RM-2L) and a 200-mL reactor (ChemiSens RM-2S).[55] These reactors are computer-controlled and data for reactor temperature, stirring speed, stirring power, evolved heat, and reactor pressure are continuously collected. In the semibatch operation, the computer can be used to control the feed rates of the monomers. The monomer feed rate can either be set at a constant value (g/min) or controlled to maintain a preset polymerization power output. Gaseous and liquid monomers can be fed to the reactor at the same time, at pressures up to 15 bars.

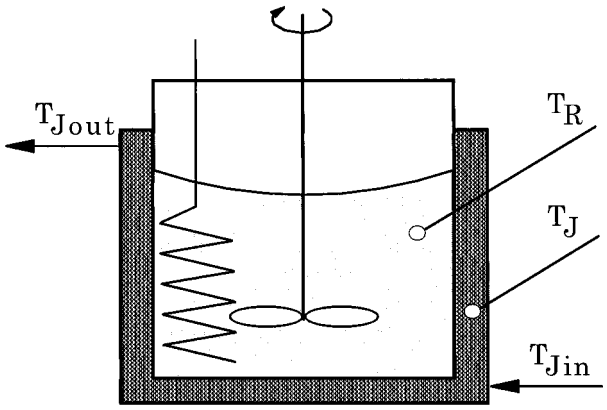

Figure 1 Schematic drawing of the calorimetric reactor showing the HF and HB measuring principles.

Reaction Calorimeter Principles

The polymerization heat is measured by two independent methods: The first is based on the principle of heat flow (HF). The power output is expressed as the HF caused by the temperature difference between the reactor and the jacket (see Fig. 1):

$$P = UA(T_R - T_J) \tag{1}$$

where T_R is the reactor temperature; T_J, the jacket medium temperature; U, the heat-transfer coefficient; and A, the heat-transfer area. The temperature difference is large and the response is fast and detailed. The value of $U \times A$, and, thus, the measured power output, depends on the stirring speed, the viscosity, the wetted area, etc., and can change significantly during an experiment. To overcome such problems, the heat-balance (HB) method was used as well. The HB method is independent of the value of $U \times A$ and utilizes the total HB of the thermostatting liquid

passing through the reactor jacket (see Fig. 1) and is expressed as

$$P = FC_p(T_{J\text{out}} - T_{J\text{in}}) \quad (2)$$

where $T_{J\text{out}}$ is the jacket medium outlet temperature; $T_{J\text{in}}$, the jacket medium inlet temperature; F, the thermostatting liquid flow rate; and C_p, the heat capacity of the thermostatting liquid. The temperature difference is small and the response is comparably slow since the heat capacities of the outer parts of the reactor are included in the measuring system. The value of $F \times C_p$ is independent of the reaction conditions, and the measured power output is thus independent of $U \times A$. By combining the measuring principles, the best properties from each system can be extracted. The HF calorimeter is fast and sensitive but cannot be universally calibrated since the value of $U \times A$ depends on the reaction conditions, while the HB calorimeter is comparatively slow, but the calibration is independent of the reaction conditions.

The HF system is calibrated before starting the reaction. By adding a pulse of known electrical power to the system, the response of the measuring system can be compared with the known energy of the pulse. In semibatch polymerization with a calibrated system, the HF and the HB signals initially have the same response. As the polymerization proceeds, an increasing difference in the responses may develop. For example, increased viscosity will decrease the heat-transfer coefficient, U, and therefore change the sensitivity factor $U \times A$ of the HF signal. This can be corrected for by assuming the deviation in the signals to be conversion-dependent. The ratio of the HB signal to the HF signal can be plotted versus the integral of the HB signal, which is proportional to the conversion. If the HB/HF ratio is continuous and does not exhibit any step changes, the curve can be approximated by a straight line, which is used for calibration. The HF signal multiplied by the corresponding HB/HF value from the calibration curve will thus give the corrected calorimetric output.

EXPERIMENTAL

Materials

Styrene (S) (Merck, Hohenbrunn, Germany; pro analysi), divinylbenzene (DVB) (Merck, pro analysi), and MAA (Merck, pro analysi) were purified by passing them through a column filled with aluminum oxide (Merck, active base). The purified monomers were stored at 4°C before use. Butadiene (B) (Air Liquide, Malmõ, Sweden; minimum 99.5%) was vacuum-distilled directly before use and passed through a column of aluminum oxide (Merck, active base). Distilled, deionized (DI) water was used. All other chemicals were of analytical grade and were used as supplied.

Table I Recipes for the PS Seed Latexes Preparation

	PS Seed Latex		
Ingredients/Conditions	A	B	C
DI water (g)	1103	1114	1130
S (g)	300.1	300.9	304.3
CCl_4[a] (g)		15.0	
DVB[b] (g)			1.25
Na_2CO_3[c] (mmol/L)	13.9	13.8	13.7
Na_2EDTA[c] (mmol/L)	1.32	1.30	1.30
SDS[c] (mmol/L)	6.85	6.79	10.1
KPS[c] (mmol/L)	2.64	2.02	2.67
Stirrer speed (rpm)	450	350	275
Polymerization time[d] (h)	2	3	5.8

[a] Added together with the monomer.
[b] Starved fed for 140.5 min after the gel peak, at a polymerization rate corresponding to 3 W heat output. DVB was added as a 4 wt % S solution, corresponding to 10 wt % of the total monomer added. During this period, a 7.54-mL degassed solution of SDS, 0.347 mol L^{-1}, was slowly added.
[c] Based on the aqueous phase.
[d] Total reaction time at 70°C, including semicontinuous monomer addition.

Preparation of Seed Latexes

Seed latexes were prepared in a 2-L pressure calorimetric reactor (ChemiSens RM-2L) using potassium persulfate (KPS) as an initiator and sodium dodecyl sulfate (SDS) as an emulsifier. The polymerization rate was measured and monitored on-line. The data were used to control monomer-charging rates and to calculate the conversion. The seed latex recipes are given in Table I.

In the preparation of seed A, S, and other chemicals, except the initiator, were charged together with the water. The reactor contents and the initiator solution were repeatedly degassed and purged with nitrogen at room temperature. The reactor was then tempered at 70°C and the calorimeter calibrated. The reaction was started

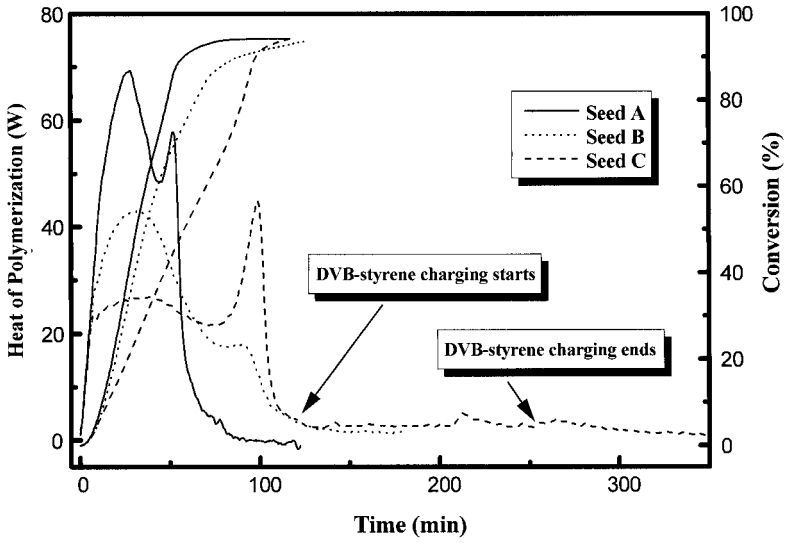

Figure 2 Polymerization rate curves for PS seed latexes. Left axis: polymerization heat. Right axis: conversion, X_M. Horizontal axis: time.

by adding the initiator solution, preheated to 70°C, through a valve. When the reaction rate had dropped to zero, the temperature was increased to 90°C and held there for 2 h. The reactor was then kept at 50°C for 5 h under vacuum suction and the contents stirred gently. Before the temperature was increased, samples were taken for gravimetric determination of the conversion. In seed B, CCl_4 [the chain-transfer agent (CTA)] was charged together with the other chemicals before polymerization was started. All other operations were as described above.

In the preparation of seed C, DVB was used as a comonomer. The polymerization was initially performed as described above, with 90% of the S monomer charged from the start. To introduce a shell containing double bonds and crosslinks in the latex particles,[36,38] the last 10% of the S monomer was mixed with 4% DVB and added by a computer-controlled pump when the polymerization rate decreased after the Trommsdorff effect. The charging rate was controlled to give a power output of 3 W (see Fig. 2, seed C). A degassed solution of SDS (7.54 mL, 0.347 mol L^{-1}) was also slowly added during charging of the monomer mixture. After addition of the monomer mixture, the reactor was kept at 70°C with an unchanged stirrer speed for 2 h. The reactor was then held at 90°C for 2 h and then at 50°C for 5 h under vacuum suction and gentle stirring. Samples were taken for gravimetric determination of the conversion before the temperature increase.

Prior to the second stage, the seed latexes were thoroughly dialyzed (membrane: Spectra/Por® MWCO: 6-8000, Spectrum Medical Industries, Inc., Houston, Texas) at ambient temperature against distilled and deionized water, containing 1.5 g SDS/L, to remove inorganic ingredients, monomers, and, in some cases, the CTA. The SDS solution was changed once every 24 h for a period of 2 weeks. After dialysis, the solid content of the latex was determined.

Second-Stage Polymerization

A 200-mL high-pressure calorimetric reactor (ChemiSens RM-2S) was used in the second stage. The polymerization rate was measured and monitored on-line. The data were used to control monomer charging rates and to calculate the conversion. A piezoelectric pressure transducer, WIKA Tronic 891.13.530, monitored the reactor pressure, with an accuracy of 0.005 bar absolute pressure. The reactor lid was heated to a temperature slightly above the reactor temperature in order to avoid condensation of B on any surfaces in contact with the vapor phase. The weight ratio (dry weight) of the seed latex (A, B, and C) and the second-stage monomer was 1 : 1. The monomers used were B, S, and MAA with a fixed S/B ratio of 1 : 1 and an MAA content of either 1 or 10 wt %. The second-stage polymerization recipes are given in Table II.

Polymerization was performed as a seeded batch process. The reactor containing seed, S, and

Table II Recipes for the Second-Stage Latexes

	Latexes					
Ingredients/Conditions	A1	B1	C1	A10	B10	C10
PS seed[a]	A	B	C	A	B	C
MAA[b] (wt %)	1	1	1	10	10	10
B[b] (wt %)	50	50	50	45	45	45
S[b] (wt %)	49	49	49	45	45	45
Na_2CO_3[c] (mmol/L)	13.7	13.6	13.6	13.6	13.6	13.4
Na_2EDTA[c] (mmol/L)	1.28	1.28	1.27	1.30	1.27	1.29
KPS[c] (mmol/L)	1.00	1.00	1.00	1.00	1.00	1.00
SDS[d] (mmol/L)	—	—	—	—	—	—
Stirrer speed (rpm)	550	550	550	550	550	550
Polymerization time[e] (h)	4.8	4.6	4.1	2.1	3.4	4.5

[a] Seed : second-stage monomer ratio (w/w) was 1 : 1 in all polymerizations.
[b] Weight percent of second-stage monomer.
[c] Based on the aqueous phase.
[d] In the second-stage polymerization, no additional SDS was added after dialysis of the seed latexes.
[e] Time required from initiation to reach a constant heat of polymerization < 0.1 W.

MAA was repeatedly degassed and purged with nitrogen at room temperature. The freshly distilled B was then charged from a weighed pressurized vessel via a computer-controlled valve and the temperature was increased to 80°C. After approximately 40 min, the temperature was stable within ± 0.05 K, and the calorimeter was calibrated. Injecting the initiator solution through a membrane into the reactor started the reaction. In some experiments, a slow autopolymerization was detected prior to injection of the initiator, which complicated the calibration. Whenever possible, the calorimetric data were corrected for autopolymerization. The final conversion was calculated from the integral of the polymerization rate curve relative to the amount of monomer charged.

DSC

Polymer films were prepared by applying latex onto clean glass plates and drying at room temperature and analyzed with a Mettler DSC 30 instrument equipped with a low-temperature cell. The film samples were first heated to 130°C at 15°C/min. After 5 min at 130°C, the samples were cooled to −150°C at a rate of 15°C/min and finally reheated to 300°C at a rate of 10°C/min. The last run was used for the determination of the T_g.

Electron Microscopy

The morphology of the latex particles was examined with a JEOL 100 U transmission electron microscope (TEM). To avoid distortion of the latex particles during drying, they were stained with osmium tetroxide in the liquid phase.[54] In the TEM micrographs, the polybutadiene (PB)-containing domains are dark, and the PS-containing domains, light gray. Average particle diameters were calculated from measurements on micrographs of OsO_4-stained latex particles.[54]

Conductometric Titration

Sulfate groups originating from the initiator and acid groups present on the second-stage latex particle surfaces were determined by conductometric titration. The latexes were ion-exchanged before titration. Latex (0.8 g) was weighed into a flask and 0.06 g of a nonionic surfactant (Dowfax 63 NIC) was added per gram polymer, in order to avoid agglomeration. Approximately 1.6 g of the mixed-bed ion-exchange resin (Bio Rad AG 501-X8, 20–50 mesh) was then added. This resin contains both anionic and cationic sites with a total capacity of 1.5 μequiv/mL. The mixture was stirred for 1–2 h and then filtered to remove the resin. To the filtrate was added 5 mL 0.01*M* HCl and 10 mL 0.01*M* NaCl to achieve a conductivity of 50 mS/cm. Distilled water was added up to a volume of 500 mL, and the mixture was sparged with nitrogen for 15 min before titration under a N_2 blanket with freshly prepared 0.01*M* NaOH. A blank titration of 5 mL 0.001*M* HCl and 10 mL 0.01*M* NaCl, diluted with distilled water to a volume of 500 mL, was carried out under similar

conditions. The blank titration was subtracted from the latex titration data. The titration curve had two inflection points, the first one corresponding to titration of the —OSO_3^- ions and the second to titration of COO^- groups.

Gel Permeation Chromatography

Gel permeation chromatography (GPC) of the seed latexes and some second-stage latexes (see Table IV) was performed with a system (Waters Associates, Milford, MA) equipped with a RI/viscosity detector (Viskotek, Model 250) and a laser light-scattering detector (LALLS, LDC Analytical, KMX-6). A set of three columns (Waters μ-Styragel, 10^5, 10^4, 10^3 Å) was used at ambient temperature. The GPC system was calibrated using six PS samples (Polymer Laboratories, Church Shetton, UK) having narrow molecular weight distributions. The THF flow rate was 1.0 mL min^{-1}. All seed latexes were dissolved in THF, and after 24 h, the samples were filtered through a 0.2-mgr;m filter, and 150 μL of this filtrate (0.003 mg mL^{-1} THF) was injected. The molecular weights presented are defined as the GPC peak value, M_{GPC}.

Table III Data for the Seed Latexes

Measurement	PS Seed Latex A	PS Seed Latex B	PS Seed Latex C
Conversion[a] at $R_{p\max}$ (%)	39.5	36.2	32.1
M_p[a] (mol/L)	5.48	5.74	6.07
Gel peak conversion[a] (%)	82.6	85.0	86.3
End conversion[b] (%)	94.9	93.6	93.9
Solid content[c] (wt %)	24.2	24.0	20.0
Particle diameter[d] (nm)	88	90	137
PDI	1.034	1.142	1.021
$M_{GPC} \times 10^{-3}$	1300	230	1350
			>4000[e]
MWD[f]	1.7	3.3	—

[a] Based on the initial amount of monomer charged.
[b] Determined before temperature was increased to 90°C (see Experimental).
[c] Determined after dialysis.
[d] The diameters reported are number averages, $\bar{D}_n$, obtained from TEM measurements.
[e] Polymer fraction above the exclusion limit of the column system.
[f] MWD = M_w/M_n. Values calculated from RI/viscometry data.

RESULTS AND DISCUSSION

Preparation of PS Seed Latexes

In the present study, PS latexes with different molecular weights and crosslinking densities were used as seeds for a second-stage polymerization of S/B. Three types of PS latexes were prepared according to the recipes and polymerization conditions given in Table I. As evident from the table, latex A was an ordinary PS latex without any modification. Latex B had a lower molecular weight because of the use of CCl_4 as a CTA in the polymerization. The polymerization conditions for latex C were initially similar to those used for latex A, but near the end of the polymerization, DVB was introduced as a comonomer under starved conditions to produce crosslinked particle shells with residual double bounds available for grafting in a subsequent seeded polymerization. The characteristics of the final seed latexes are given in Table III.

Because of problems with latex stability, a lower stirring speed had to be used in the preparation of latexes B and C, compared with latex A (see Table I). Despite this difference, latexes A and B had similar particle sizes, 88 and 90 nm, respectively. Latex C, however, had larger particles (137 nm). The broader particle-size distribution shown by latex B compared to that of A and C, as seen in Table III, may be an effect of the CTA used, but the role of CTAs in emulsion polymerization is presently unclear.

The molecular weights of the seed latex polymers were analyzed with GPC using RI, LALLS, and viscometry detectors (see Experimental). Peak molecular weights obtained from the LALLS detector (M_{GPC}) are given in Table III. The value for seed B was approximately six times lower than that of seed A and the molecular weight distribution (MWD) broader. The higher MWD value obtained for seed B is probably an effect of the CTA. As the polymerization proceeds in a batch process, the CTA will be consumed, leading to an increase in the instantaneous molecular size and a broadening of the MWD.[56]

According to the GPC results, latex C, which contained particles with a crosslinked shell, had a polymer fraction with a molecular weight similar to that of the polymer in latex A. This fraction should correspond to the initially formed homo-PS core. The LALLS detector detected another

polymer fraction, which presumably consisted of microgel derived from the DVB-containing shell. The apparent molecular weight was greater than 4,000,000, which is above the exclusion limit of the column system used.

Styrene Polymerization Kinetics

The curves given in Figure 2 represent the heat energy generated by the polymerization of S at 70°C, as measured by the calorimetric reactor, and the calculated conversion, X_M, of the monomer added. The final conversions given in Table III were determined gravimetrically after the reaction had ended and were, in all cases, close to 95%.

In the preparation of latex C, the addition of DVB at the end of the polymerization should lead to polymerization of DVB at the surface of the PS particles. To achieve this goal, polymerization should proceed under starved conditions and, thus, the feeding rate of the S/DVB mixture was controlled to give a heat flow of only 3 W (cf. Fig. 2). The GPC analyses point at a two-phase particle morphology for latex C, presumably consisting of a crosslinked shell and a core of unmodified PS.

The polymerization kinetics of experiments A, B, and C were compared. To obtain a valid comparison, the X_M values for seed C were recalculated relative to the amount of monomer initially charged, that is, 90% of the total.

As can be seen in Figure 2, the values for the maximum reaction rate, $R_{p\max}$, differed in the three experiments, presumably as an effect of the different stirring speeds.[57] According to the familiar Smith–Ewart terminology,[58] $R_{p\max}$ corresponds to the onset of stage III in emulsion polymerization.[59] The monomer concentration in the particles, M_p, at $R_{p\max}$ can be calculated from the corresponding monomer conversion, and the present results are given in Table III. It can be noted that Harada et al.[60] reported that X_M = 43% in the emulsion polymerization of S at 50°C, and under similar conditions, Varela De La Rosa et al.[59] obtained X_M = 38% at $R_{p\max}$. The present values were in the expected range for latexes A and B, but for latex C, X_M was lower and M_p higher than those reported in the literature (Table III).

The M_p values reported by Harada et al.[60] and Varela De La Rosa et al.[59] were 5.48 (onset stage III) and 5.62 mol L^{-1} (at $R_{p\max}$), respectively. It can be noted that in a series of nine S polymerizations performed under conditions similar to those used for latex A, we found an average value of 36.1 ± 4.6% for X_M at $R_{p\max}$, corresponding to M_p = 5.75 ± 0.37 mol L^{-1}.

Large differences were observed in the heat evolved during the Trommsdorff effect, that is, the gel peak, as can be seen in Figure 2. Latex B, having the lowest molecular weight, had a significantly lower gel peak height, relative to the first maximum, than those of latexes A and C. The largest gel peak was obtained for latex C, which had the largest particles. A decrease in the number of polymer particles and a corresponding increase in the particle size gave a significant increase in the average number of radicals per particle due to slow termination and, therefore, a large increase in the rate of polymerization. In other words, the larger the particle volume and the smaller the number of polymer particles, the greater the acceleration in the rate of polymerization due to the gel effect.[61] The observed results are in line with results published by Varela De La Rosa et al.,[59] who obtained a flatter polymerization heat curve and a more significant second maximum on decreasing the emulsifier concentration and increasing the particle size. They found that the gel peak occurred between 82 and 84% conversion at 50°C. In the present investigation, the gel peaks were observed at slightly higher conversions (Table I), which can be expected for polymerization at 70°C due to the increase in the polymer diffusion rate. However, the observed differences are small.

Second-Stage Polymerization

The aims of this work were to prepare heterogeneous film-forming S/B latex particles and to study how the properties of the seed particles influenced the second-stage polymerization and the final morphology of the heterogeneous particles. The second phase consisted of (S/B/MAA) with an S/B weight ratio of 1 : 1 and an MAA content of either 1 or 10 wt %. Polymerization was run as a seeded batch process with a weight ratio of 1 : 1 between the seed and the second-phase polymer, using the PS latexes A, B, and C as seeds. The polymerization recipes are given in Table II. The final latexes had unimodal, narrow particle-size distributions when latexes A and C were used as seeds, while those prepared from latex B had a broader particle-size distribution reflecting that of the seed particles.

Some of the latexes were analyzed with GPC, despite some fractions of the polymers not being

Table IV Data for the Second-Stage Latexes

Measurement	Latexes					
	A1	B1	C1	A10	B10	C10
End conversion[a] (%)	94.1	100	99.6	98.0	87.7	95.4
Solid content[b] (wt %)	31.3	32.6	31.7	31.7	29.9	31.2
Particle diameter[c] (nm)	125	135	188	120	120	179
PDI	1.029	1.053	1.016	1.034	1.098	1.014
T_g soft phase (°C)	−24	−39	−33	7	6	9
T_g hard phase (°C)	102	97	104	103	101	102
—COO^- [d] (%)	18	19	29	8	6	4
$M_{GPC} \times 10^{-3}$	—	260	1700 + >4000[e]	—	230	1780 + >4000[e]
Crosslink onset (% conversion)	—	69	57	—	—	45

[a] Gravimetrically determined. Sample taken before vacuum suction of residual monomers.
[b] Determined after vacuum suction of residual monomers.
[c] The diameters reported are number averages, $\bar{D}_n$, obtained from TEM measurements using OsO_4 staining.[54]
[d] Determined by conductometric titration. Presented as the percentage of acid groups found in relation to the total amount charged.
[e] Polymer fraction above the exclusion limit of the column system.

soluble in THF due to crosslinking. The molecular weights given in Table IV are therefore to be regarded only as indications of the molecular sizes of the soluble fractions. Nevertheless, some important observations can be made: The latexes prepared from latex C, which had a slightly crosslinked shell, all contained a microgel fraction with a size small enough to pass through a 0.45-μm filter, but larger than the exclusion limit of the column. These latexes also had a soluble fraction presumably originating from the PS core in the seed particles. The heterogeneous latexes based on latex B, which had a reduced molecular weight due to the use of a CTA, all had second-stage polymers with low molecular weights. Additional analysis of latex B by gas chromatography–mass spectrometry (purge and trap GC–MS) showed that residual amounts of CCl_4 were present, even though the latex had been thoroughly dialyzed. As a consequence, the residual CCl_4 had acted as a CTA also in the second-stage polymerization, reducing the molecular weight of the second-stage polymer.

The heterogeneous latexes prepared were all film-forming. The film morphologies and their dynamic mechanical properties were presented and discussed elsewhere.[24] In the present work, we investigated the thermal properties of the latex films with DSC. The results of these measurements are presented in Table IV, and they clearly show that the polymer particles consist of two phases having different glass transition temperatures. The transition observed at approximately 100°C can be ascribed to the PS seed phase, while the second transition, which varied from −39°C to +15°C depending on the polymer composition and the type of seed used, can be attributed to the second-stage polymer. It can be noted from Table IV that latexes containing 1 wt % MAA in the second-phase polymer had different values of T_g even though the polymers should have similar compositions according to the recipe. In the latexes containing 10 wt % MAA in the second phase, no corresponding differences in T_g were detected. The differences in T_g for latexes with 1 wt % MAA can be attributed to differences in the second-stage polymer molecular weights. However, in the polymers containing 10 wt % MAA as a comonomer, the increase in T_g due to the presence of the MAA units in the chains dominated the effects of the molecular weight.

Second-Stage Polymerization Kinetics

Second-stage polymerization was performed as a seeded batch process. The reactions were monitored by measuring the heat output from the polymerization and the reactor pressure. In Figure 3, the heat output is plotted against the conversion of the second-phase monomers (X_M) in the

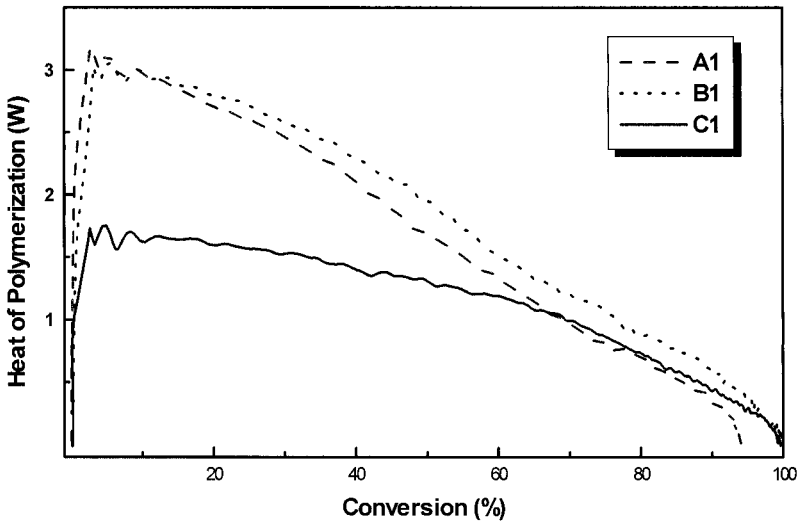

Figure 3 Second-stage polymerization rate curves for 1 wt % MAA copolymer latexes: A1, B1, and C1. The polymerization heat is plotted as a function of the conversion, X_M.

preparation of the latexes A1, B1, and C1. The S/B monomer mixture contained 1 wt % MAA. As is evident from the figure, the curves from the preparation of latexes A1 and B1 were almost identical in shape, showing a peak polymerization rate at low conversion followed by a gradual decrease. The curve from latex C1 shows no peak in the reaction rate. The heat-flow curve was flat and the major part of the polymerization occurred at a constant reaction rate up to a conversion of 65%; thereafter, the rate slowly decreased. The polymerization time, that is, the time measured from initiation to the point when the heat flow was less than 0.1 W, was identical in the preparation of latexes A1 and B1, while it was slightly shorter for latex C1 due to the higher average polymerization rate. The end conversions in all three polymerizations were higher than 90% (Table IV).

The heat-flow curves obtained from the preparation of latexes A10, B10, and C10, all containing 10% MAA as a comonomer in the second

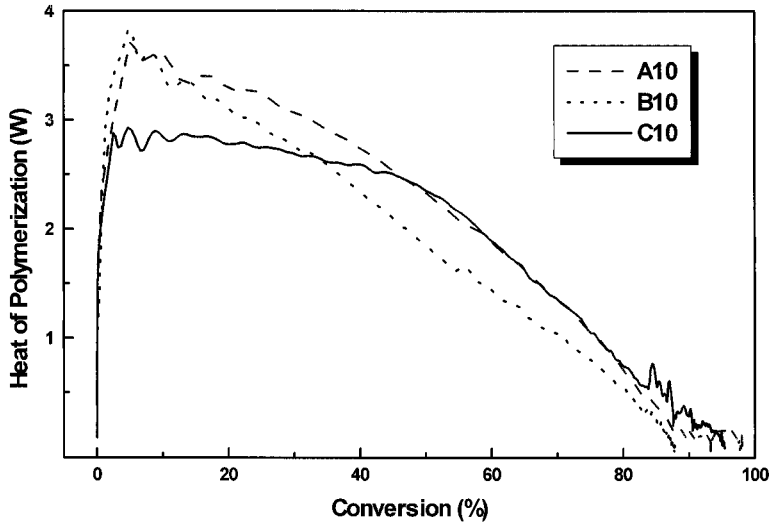

Figure 4 Second-stage polymerization rate curves for 10 wt % MAA copolymer latexes: A10, B10, and C10. The polymerization heat is plotted as a function of conversion, X_M.

stage, are shown in Figure 4. The polymerization rates were significantly higher than in the case of 1 wt % MAA. The higher rates may be due to a catalytic effect related to the presence of MAA, which was reported by Shoaf and Poehlein[62] for emulsion polymerization of S/MAA. Furthermore, the carboxylic groups will decrease the interfacial energy of the particles. This may lead to a higher concentration of the monomer in the latex particles,[63] thereby resulting in a correspondingly higher rate of polymerization.[64]

However, the general shapes of the polymerization curves were similar for the two levels of MAA. Latexes A10 and B10 gave almost identical curves when plotting heat output versus X_M, while for latex C10, a constant polymerization rate up to approximately 50% conversion was observed (see Fig. 4). The final conversions are given in Table IV. Because of the higher reaction rates, the polymerization times, defined as above, were much shorter for latexes A10 and B10 than for the corresponding experiments with 1 wt % MAA, that is, 2 and 3.4 h, respectively. However, latex C10 continued to polymerize at a low rate, giving a polymerization time of 4.5 h.

The differences in MW for latexes prepared from seeds A and B were not accompanied by any differences in the second-stage polymerization rates. No initial period of constant reactor pressure was observed in any of these second-stage polymerizations, which indicated that no free monomer phase was present. However, the low, broad second-stage polymerization curves connected to seed C probably are a result of the large particle size of seed C and, hence, the low number of particles per volume. At higher conversions, where the polymer mobility will be restricted due to high internal viscosity, due to monomer depletion, polymerization curves coincide with those from seed A and seed B.

Due to their hydrophilicity, the acid groups will accumulate at the particle surface, provided the mobility of the polymer phase allows reorientation. Conductometric titration was used to provide information on the location of the acid groups, that is, the carboxylic acid groups and the comparatively small amounts of sulfonic acid groups derived from the initiation. The amounts of acid groups found in the titrations are given in Table IV as the fraction of initially charged acid groups. The results may be divided into two categories: The first group contains latexes prepared with 1 wt % MAA. In this group, between 18 and 29% of the charged acid groups are found at the surfaces of the particles. The second group consists of the latexes prepared with 10 wt % MAA. In this category, between 4 and 8% of the charged acid groups were found at the particle surface, which leads to a concentration of acid groups at the particle surface which is much higher than in the case of 1 wt % MAA.

Crosslink Conversion

As the monomer concentration in the particles decreases, the probability of chain transfer to the polymer and crosslinking reactions increases. It was pointed out by Tobita[65] that on increasing the crosslink density of the particles the elastic contribution to the free energy for the polymer/monomer system would increase and the equilibrium monomer concentration in the particles, consequently, decrease. In the present system, it was observed that the reactor pressure, which decreased linearly as a function of conversion, showed an irregularity which may be interpreted as a "squeezing out" of monomer from the particles, in accordance with the crosslinking effect described by Tobita. The effect is shown for latex C1 in Figure 5. According to the figure, the monomer was consumed in the region 55–70% conversion with very little change in the reactor pressure, leading to a displacement of the pressure curve toward higher pressures. The crosslinking effect onset was in some second-stage polymerization processes difficult to observe. In some polymerizations, the slope of the curve changed but no irregularity, as shown in Figure 5, was observed.[66] For those cases, no values are reported. The average value obtained for the crosslinking onset conversion was 56 $\pm$ 15%. Conversion values for the onset of the crosslinking effect are given in Table IV.

Particle Morphologies

The morphologies of the heterogeneous particles were studied by TEM after staining with osmium tetroxide. TEM micrographs for latexes A1 and B1 are shown in Figure 6(A,B). Both latexes have hemispherical particle morphologies of similar appearance. However, the phase separation in latex B1 seems to be more pronounced. The particles in B1 are composed of two hemispheres, compared with the acornlike structures in latex A1. As noted above, the polymerization rates were similar in the preparation of the latexes. The morphological differences may thus be ascribed to

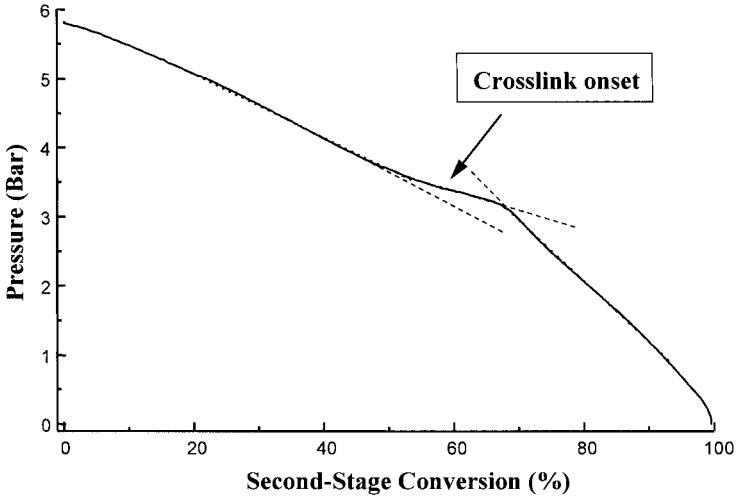

Figure 5 Monomer pressure plotted as a function of conversion X_M in stage two, showing the principle for the detection of the crosslinking interval for latex C1.

differences in molecular weight between the two latexes. The internal particle viscosity during the second-stage polymerization would thus be lower in latex B1 than in latex A1.

In Figure 6(C), a micrograph of latex C1 is shown. These latex particles had a morphology that can be described as an occluded simplified hemisphere (SHSOCC).[49] Several occlusions of different sizes of the second-stage polymer were distributed in the seed polymer matrix. This morphology may be the result of several factors. The large second-stage-polymer domain seen in the particles in Figure 6(C) is the result of polymerization inside the particles early in the second stage of polymerization. As seen in the Figure 6(A), the equilibrium morphology is hemispherical and it is thus likely that the initial low viscosity in the particles will promote the formation of a large second-phase polymer domain in the particles. At higher conversions, the effect of crosslinking will contribute to the particle morphology. The contribution from the elastic free energy can, even at low crosslinking levels, dominate the evolution of the particle morphologies.[41,52]

Latex A10, B10, and C10 particles undoubtedly all have the second-stage polymer exposed to the water phase, as shown in the TEM micrographs in Figure 7(A–C). The micrographs for latexes A1, B1, and C1 can, on the other hand, be interpreted as the particles have thin shells consisting of the seed phase (Fig. 6). The micrographs show a lightly colored phase surrounding the darker second-stage phase domains in the particles. This outer lightly colored phase cannot be observed in the micrographs from latexes A10, B10, and C10. This difference, however, may be an artifact.

In an earlier study,[14] we demonstrated the development of the particle morphology when increasing the acid content in seeded polymerization using poly(isoprene-*co*-methacrylic acid) as the second-stage polymer. When the acid content of the polymer increased, the second-stage polymer increasingly accumulated at the aqueous phase, with formation of a thin shell of a hydrophilic polymer. In the present investigation, the particle morphologies displayed a similar development on increasing the acid content of the second-stage polymer. As shown by Figure 7(A,B), the particle morphologies for latexes A10 and B10 were similar.

For both latexes, the particles display core–shell morphologies, with the second-stage polymer surrounding the seed polymer particles. In latex A10, the hydrophilic shell is generally thinner and covers more of the original seed particles than in latex B10. This difference is probably a consequence of the reduced molecular weight in latex B10. However, the morphological difference between latexes A10 and B10 is much less pronounced than for latexes A1 and B1. The hydrophilic properties of the second phase obviously dominate over the effects of molecular weight at high acid contents in determining the particle morphology.

As shown in Figure 7(C), latex C10 has a particle morphology corresponding to an occluded hemispherical type, similarly to latex C1. The large domain in the particles, consisting of the

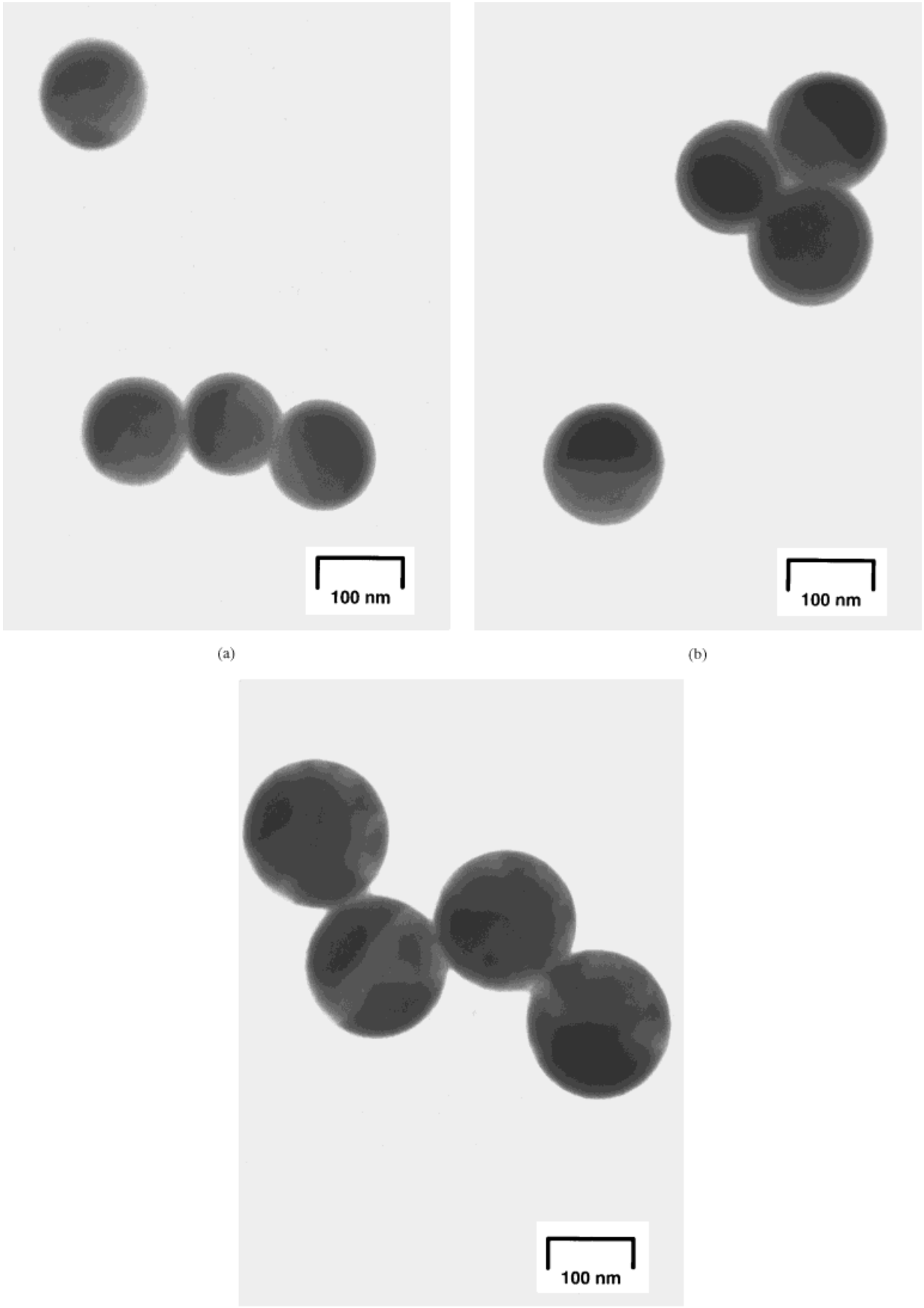

(a) (b) (c)

Figure 6 TEM micrographs showing the particle morphology of latexes: (a) A1; (b) B1; (c) C1.

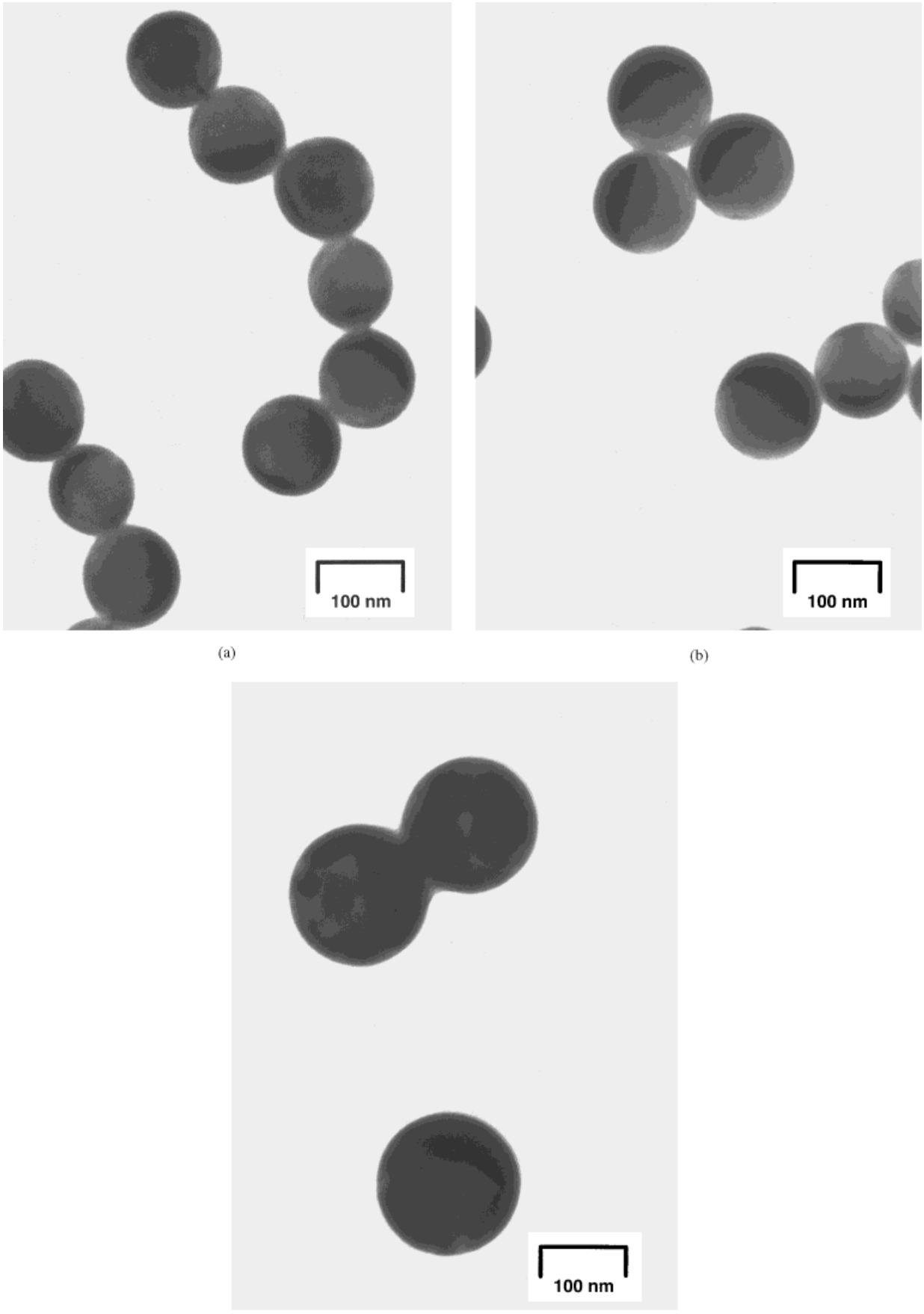

(a) (b) (c)

Figure 7 TEM micrographs showing the particle morphology of latexes: (a) A10; (b) B10; (c) C10.

second-stage polymer, has a different appearance in latex C10 than that in C1. In C10, the second-stage domain is located outside the original seed particle, trying to grasp it, having a first-quarter moon-shape. In latex C1, the large domain, having a hemispherical shape, seems to be located near the particle surface and surrounded by the seed polymer. The similarity in the two morphologies and in the kinetic behavior suggests that the two latexes polymerize by similar mechanisms, at least initially. However, because of the more hydrophilic nature of the second-stage polymer in latex C10, it will have a strong tendency to accumulate at the particle surface.

CONCLUSIONS

The use of a calorimetric reactor to monitor and control emulsion polymerization provides the opportunity to study reaction kinetics and to tailor latex formation. In the preparation of the PS seed latexes at 70°C, the conversion at $R_{p\max}$ was found to be particle-size-dependent. The Trommsdorff effect occurred at conversions between 83 and 86% and the heat evolved during the Trommsdorff effect was found to be dependent on the molecular weight of the polymers and the particle size as well as the number of particles per unit volume. In the second polymerization stage, differences in the polymerization reaction rates were found when the amount of MAA in the second-phase polymer composition was altered. The MAA had a promoting effect on the polymerization rate, and polymerizations performed with a higher amount MAA present were faster than were the corresponding experiments with low MAA content.

Due to crosslinking of the copolymer formed in second-stage polymerization, the equilibrium concentration of the monomer in the particles decreased with time, which could be detected as a change in the slope in the curve relating pressure and conversion. This phenomenon defined the conversion at which the onset of crosslinking of the second-stage polymer occurred.

Latex particle morphologies could be related to the molecular weights of the seed latex polymers when the acid content in the second-stage copolymer was low. At high acid content in the second-stage polymer, the effects of the hydrophilic acid overrode the molecular weight effects and controlled the development of the core–shell morphology in the particles. The effects of crosslinking of the seed latex dominated the morphology at all levels of the acid monomer in the second-stage polymer.

The authors gratefully acknowledge the financial support of this work by the Swedish Research Council for Engineering Sciences, TFR. The authors also thank Bodil Wesslén for her assistance with the GPC analyses and Elly Westberg at MoDo AB for her kind help with the conductometric titration.

REFERENCES

1. Taber, D. A.; Stein, R. C. Tappi J 1957, 40, 107.
2. Van Gilder, R. L.; Purfeerst, R. D. In TAPPI Coatings Conferecne Proceedings, 1994; p 229.
3. Lee, D. I. In TAPPI Coatings Conference Proceedings, 1982; p 125.
4. Rigdahl, M.; Lason, L.; Hagen, R.; Karlsson, O.; Wesslen, B. J Appl Polym Sci 1997, 63, 661.
5. Grancio, M. R.; Williams, D. J. J Polym Sci A-1 1970, 8, 2617.
6. Matsumoto, T.; Okubo, M.; Shibao, S. Kobunshi Ronbunshu Eng Ed 1976, 5, 784.
7. Okubo, M.; Katsuta, Y.; Matsumoto, T. J Polym Sci Polym Lett Ed 1980, 18, 481.
8. Okubo, M.; Ando, M. Yamada, A.; Katsuta, Y.; Matsumoto, T. J Polym Sci Polym Lett Ed 1981, 19, 143.
9. Okubo, M.; Katsuta, Y.; Matsumoto, T. J Polym Sci Polym Lett Ed 1982, 20, 45.
10. Okubo, M.; Kanaida, K.; Matsumoto, T. Coll Polym Sci 1987, 265, 876.
11. Okubo, M.; Murakami, Y.; Tsukuda, Y. Chem Express 1993, 8, 253.
12. Stutman, D. R.; Klein, A.; El-Aasser, M. S.; Verhoff, J. W. Ind Eng Chem Prod Res Dev 1985, 24, 404.
13. Lee, D. I.; Ishikawa, T. J Polym Sci Polym Chem Ed 1983, 21, 147.
14. Karlsson, O.; Hasser, H.; Wesslén, B. J Appl Polym Sci 1997, 63, 1543.
15. Lambla, M.; Schlund, B.; Lazarus, E.; Pith, T. Makromol Chem Suppl 1985, 10/11, 463.
16. Cavaille, J. Y.; Jourdan, C.; Kong, X. Z.; Perez, J.; Pichot, C.; Guillot, J. Polymer 1986, 27, 693.
17. O'Connor, K. M.; Tsaur, S.-L. J Appl Polym Sci 1987, 33, 2007.
18. Zosel, A.; Heckmann, W.; Ley, G.; Mächtle, W. Coll Polym Sci 1987, 265, 113.
19. Zosel, A.; Heckmann, W.; Ley, G.; Mächtle, W. Adv Org Coat Sci Tecnhol 1989, 11, 15.
20. Richard, J.; Maquet, J. Polymer 1992, 33, 4164.
21. Hidalgo, M.; Cavaille, J. Y.; Guillot, J.; Guyot, A.; Pichot, C.; Rios, L.; Vassoille, R. Coll Polym Sci 1992, 270, 1208.
22. Hidalgo, M.; Cavaille, J. Y.; Guillot, J.; Guyot, A.; Perez, J.; Vassoille, R. J Polym Sci Part B Polym Phys 1995, 33, 1559.

23. Arora, A.; Daniels, E. S.; El-Aasser, M. S. J Appl Polym Sci 1995, 58, 301.
24. Hagen, R.; Salmen, L.; Karlsson, O.; Wesslén, B. J Appl Polym Sci 1996, 62, 1067.
25. Okubo, M.; Yamada, A.; Matsumoto, T. J Polym Sci Polym Chem Ed 1980, 16, 3219.
26. Muroi, S.; Hashimoto, H.; Hosoi, K. J Polym Sci Polym Chem Ed 1984, 22, 1365.
27. Cho, I.; Lee, K.-W. J. Appl Polym Sci 1985, 30, 1903.
28. Dimone, V. L.; El-Aasser, M. S.; Verhoff, J. W. Polym Mater Sci Eng 1988, 58, 821.
29. Hergeth, W.-D.; Brittrich, H.-J.; Eichhorn, F.; Schenkler, S.; Schmutzler, K.; Steinau, U.-J. Polymer 1989, 60, 1913.
30. Zosel, A.; Heckmann, W.; Ley, G.; Mächtle, W. Makromol Chem Macromol Symp 1990, 35/36, 423.
31. Rios, L.; Hidalgo, M.; Caville, J. Y.; Guillot, J.; Guyot, A.; Pichot, C. Coll Polym Sci 1991, 269, 812.
32. Lee, S.; Rudin, A. J Polym Sci Part A Polym Chem 1992, 30, 865.
33. Lee, S.; Rudin, A. J Polym Sci Part A Polym Chem 1992, 30, 2211.
34. Lee, D. I. In ACS Symposium Series 165; Basset, D. R.; Hamielec, A. E., Eds.; American Chemical Society: Washington, DC, 1981; p 405.
35. Jönsson, J.-E. L.; Hasser, H.; Jansson, L. H.; Törnell, B. Macromolecules 1991, 24, 126.
36. Jönsson, J.-E.; Hasser, H.; Törnell, B. Macromolecules 1994, 27, 1932.
37. Jönsson, J.-E.; Hasser, H.; Törnell, B., to be published.
38. Daniels, E. S.; El-Aasser, M. S.; Klein, A.; Verhoff, J. W. Polym Mater Sci Eng 1988, 58, 1104.
39. Lee, S.; Rudin, A. Makromol Chem Rapid Commun 1989, 10, 655.
40. Laferty, S.; Piirma, I. In ACS Symposium Series 492; Daniels, E. S.; Sudol, D.; El-Aasser, M. S., Eds.; American Chemical Society: Washington, DC, 1992; p 255.
41. Durant, Y. G.; Sundberg, E. J.; Sundberg, D. C. Macromolecules 1997, 30, 1028.
42. Torza, S.; Mason, S. G. J Coll Interf Sci 1970, 33, 67.
43. Berg, J., Sundberg, D. C.; Kronberg, B. Polym Mater Sci Eng 1986, 54, 367.
44. Waters, J. A. Eur Patent Appl EP 327 199, 1989.
45. Sundberg, D. C.; Casacca, A. P.; Pantazopoulos, J.; Muscato, M. R.; Kronberg, B.; Berg, J. J Appl Polym Sci 1990, 41, 1425.
46. Chen, Y.-C.; Dimone, V.; El-Aasser, S. M. J Appl Polym Sci 1991, 42, 1049.
47. Lee, S.; Rudin, A. In ACS Symposium Series 492; Daniels, E. S.; Sudol, D.; El-Aasser, M. S., Eds.; American Chemical Society: Washington, DC, 1992; p 234.
48. Chen, Y.-C.; Dimone, V.; El-Aasser, M. S. Macromolecules 1991, 24, 3779.
49. Winzor; C. L.; Sundberg, D. C. Polymer 1992, 33, 3797.
50. Sundberg, E. J.; Sundberg, D. C. J Appl Polym Sci 1993, 47, 1277.
51. Waters, J. A. Coll Surf A Phys Chem Eng Asp 1994, 83, 167.
52. Durant, Y. G.; Sundberg, E. J.; Sundberg, D. C. Macromolecules 1996, 29, 8466.
53. Hassander, H.; Karlsson, O.; Wesslén, B. In ICEM 13-PARIS, July 17–22, 1994; p 1215.
54. Karlsson, O.; Hassander, H.; Wesslén, B. Coll Polym Sci 1995, 273, 496.
55. Nilsson, H.; Silvergren, C.; Törnell, B. Chem Scr 1982, 19, 164.
56. Gilbert, R. G. In Emulsion Polymerization. A Mechanistic Approach; Ottewill, R. H.; Rowell, R. L., Eds.; Academic: London, 1995.
57. Nomura, M.; Harada, M.; Eguchi, W.; Nagata, S. J Appl Polym Sci 1972, 16, 835.
58. Smith, W. V.; Ewart, R. W. J Chem Phys, 1948, 16, 592.
59. Varela De La Rosa, L., Sudol, E. D.; El-Aasser, M.; Klein, A. J Polym Sci Part A Polym Chem 1996, 34, 461.
60. Harada, M.; Nomura, M.; Kojima, H.; Eguchi, W.; Nagata, S. J Appl Polym Sci 1972, 16, 811.
61. Friis, N.; Hamielec, A. E. In ACS Symposium Series 24; Piirma, I.; Gardon, J. L., Eds.; American Chemical Society: Washington, DC, 1976; p 82.
62. Shoaf, G. L.; Poehlein, G. W. J Appl Polym Sci 1991, 42, 1213.
63. Morton, K.; Kaizerman, S.; Altier, M. W. J Colloid Sci 1954, 9, 300.
64. Yeliseyeva, V. I.; Petrova, S. A.; Zuikov, A. V. J Polym Sci Part C 1973, 42, 63.
65. Tobita, H. Macromolecules 1992, 25, 2671.
66. Meehan, E. J. J Am Chem Soc 1949, 71, 628.